The Astrophysical Journal Letters, 768:L22 (5pp), 2013 May 1 doi:10.1088/2041-8205/768/1/L22
© 2013. The American Astronomical Society. All rights reserved. Printed in the U.S.A.

KINEMATICS OF THE INTERMEDIATE-MASS BLACK HOLE CANDIDATE HLX-1

Roberto Soria[1], George K. T. Hau[2], and Manfred W. Pakull[3]
[1] International Centre for Radio Astronomy Research, Curtin University, GPO Box U1987, Perth, WA 6845, Australia; roberto.soria@icrar.org
[2] European Southern Observatory, Alonso de Cordova 3107, Santiago, Chile; ghau@eso.org
[3] Observatoire Astronomique de Strasbourg, UMR 7550, Université de Strasbourg, 11 rue de l'Université, F-67000 Strasbourg, France; manfred.pakull@astro.unistra.fr
Received 2013 January 11; accepted 2013 April 5; published 2013 April 19

ABSTRACT

We studied the optical spectrum of HLX-1 during its latest outburst, using the FORS2 spectrograph on the Very Large Telescope. We detect an Hα emission line centered at $\lambda = 6718.9 \pm 0.9$ Å and find that its projected radial velocity with respect to the nucleus of ESO 243−49 is 424 ± 27 km s^{-1}, while the maximum rotational velocity of the stars in that galaxy is ≈209 km s^{-1}. This suggests that HLX-1 and its surrounding stars were not formed in situ, but came either from a disrupted dwarf galaxy or from a nuclear recoil. We also find that the Hα emission line is resolved with FWHM ≈400 km s^{-1}, suggesting a nebular rather than disk origin for the emission. Its luminosity ($L_{\mathrm{H}\alpha} \approx$ a few 10^{37} erg s^{-1}, equivalent width ≈70 Å) is also consistent with emission from a nebula photoionized by HLX-1.

Key words: accretion, accretion disks – black hole physics – galaxies: clusters: individual (Abell 2877) – galaxies: individual (ESO 243−49)

Online-only material: color figures

1. INTRODUCTION

The transient point-like X-ray source 2XMM J011028.1−460421 (HLX-1) has been interpreted as the first robust example of the long-sought class of intermediate-mass black holes (IMBHs; Farrell et al. 2009; Wiersema et al. 2010; Davis et al. 2011; Servillat et al. 2011). HLX-1 is seen in the sky inside the D25 isophote of the S0/a galaxy ESO 243−49 (heliocentric redshift $z = 0.0224$, cosmology-corrected (Planck Collaboration 2013) luminosity distance ≈99 Mpc, distance modulus ≈35.0 mag), at a distance of $\approx 8'' \approx 3.7$ kpc from the nucleus. Its peak X-ray luminosity $\approx 10^{42}$ erg s^{-1} requires a black hole (BH) mass $\gtrsim$ a few $10^3\ M_\odot$, to be consistent with the Eddington limit; this is too massive to be the outcome of a stellar collapse. This mass estimate is consistent with the values obtained from spectral modeling of the soft X-ray component, interpreted as thermal emission from an accretion disk (Farrell et al. 2009; Davis et al. 2011; Servillat et al. 2011). Its X-ray spectral variability and radio flares (Farrell et al. 2009; Godet et al. 2009; Servillat et al. 2011; Webb et al. 2012) are consistent with the canonical state transitions and jet properties of an accreting BH. The periodic nature of the X-ray outbursts (every ≈370 days) suggests that the BH is accreting from a single donor star on a very eccentric orbit (Lasota et al. 2011; Soria 2013). Explaining the origin of HLX-1 may provide the key for finding further examples of IMBHs in the nearby universe, and for understanding their role in the history of galaxy evolution.

HLX-1 has a blue optical counterpart ($B \sim V \sim 24$ mag near the outburst peak; Farrell et al. 2012; Soria et al. 2012, 2010) with Hα emission (Wiersema et al. 2010). We have studied the optical counterpart with the FORS2 spectrograph on the European Southern Observatory (ESO)'s Very Large Telescope (VLT) in 2012. In this Letter, we present the main results of our observations and discuss their implications for the nature of HLX-1.

2. OBSERVATIONS

2.1. Our 2012 VLT/FORS2 Campaign

We observed HLX-1 during its 2012 X-ray outburst (Godet et al. 2012), with VLT/FORS2 (ESO Program 088.D-0974). Spectra covering the *R* and *I* bands were taken during the nights of 2012 August 26, 27 and September 10 (total exposure time ≈3.77 hr) with the red-sensitive MIT CCDs. We used the 300I grism with 1″ slit and OG590 order-sorting filter. The median seeing estimated from the telescope's active optics was ≈0.″99, 0.″78, and 0.″70 for the three nights, respectively. The observations were made in blocks of 3×754 s exposures, with a spatial offset between each exposure to facilitate cosmic-ray and bad pixel removal. See Table 1 for a summary of the instrumental configuration.

Owing to its faintness, HLX-1 is not directly visible in the FORS2 acquisition images; therefore, we used an unresolved star-like object 9.″13 from our target for alignment (Figure 1), and oriented the slit at a position angle of 71.°9 (from north to east). We calculated this value from our previously obtained, astrometrically calibrated VLT/VIMOS images (Soria et al. 2012) and we verified it using the public archive *Hubble Space Telescope* (*HST*) Wide Field Camera 3 images. During our observations, the telescope was nodded along the slit to help us remove CCD artifacts.

2.2. VLT/FORS2 2009 Data

We also re-analyzed the archival FORS2 data taken over three nights in 2009 December (Wiersema et al. 2010). The instrumental setup was similar to that used for our 2012 observations, except for the following details. The observations were a sequence of 600 s exposures (total exposure time ≈2 hr). The alignment was done by placing the slit through two alignment stars, with a slit position angle of −70.°5. Using a public archive *HST* image, we note that with this position angle, HLX-1 was

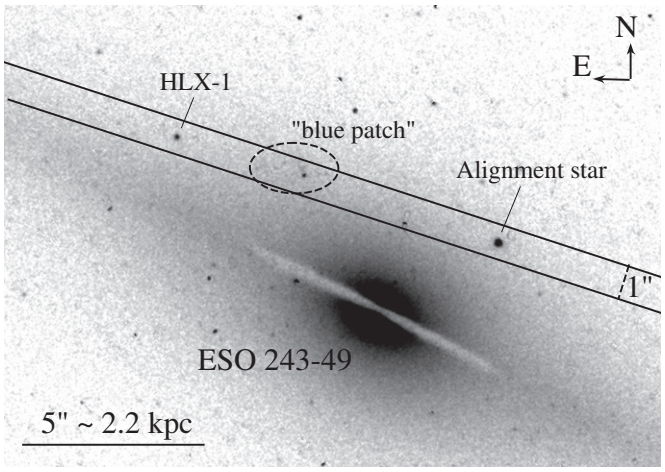

Figure 1. Slit geometry during our VLT/FORS2 observations, plotted on a gray scale *HST*/WFC3 image in the F390W band. The FORS2 spectrograph was rotated such that the 1″ slit covered HLX-1, the alignment star, and what we called "blue patch," an extended background source particularly prominent in the far-UV.

Table 1
Instrument Configuration for Program 088.D-0974(B)

Parameter	Value
Epoch	2012 Aug 27 (08:16–09:36 UT)
	2012 Aug 28 (06:28–07:48 UT)
	2012 Sep 11 (06:19–07:39 UT)
Grism	300I
Slit width	1.″0
CCD	MIT
Read noise (e^-)	2.9
Gain (e^-/ADU)	0.70
Readout mode	100 Kps/2ports/high_gain
Slit P.A. on sky	71.°9

centered ≈0.″17 off the middle of the slit toward the blue side. For the seeing ≈0.″6–0.″7 recorded on those nights, we estimate that this positional shift would cause an apparent blueshift ∼60–80 km s^{-1} of the Hα emission component with respect to the stellar absorption component (which has no offset because the stellar emission fills the slit). Thus, combining the 2009 and 2012 data sets increases the signal-to-noise ratio of the emission line, but also the error in the central position and line width.

3. DATA ANALYSIS

We followed the standard steps for the reduction of long-slit spectral data (see, e.g., Hau et al. 1999, 2009; Hau & Forbes 2006): the data were bias-subtracted and flat-fielded with a normalized internal flat. We obtained a wavelength solution using the sky emission lines in the individual spectra, ensuring optimal wavelength precision. The rms for the wavelength solutions is 0.8 Å. We modeled and subtracted the background sky spectra by fitting the sky along the spatial direction column by column, excluding regions close to ESO 243−49. We then spatially aligned and median-combined the data to reject pixels affected by cosmic rays. We created two separate two-dimensional (2D) spectra from the co-added 2009 and 2012 observations, and another one with both data sets combined, to increase the signal-to-noise ratio of the emission line. We also inspected the Hα line profiles from individual nights in 2012, but the signal-to-noise ratio is not high enough to determine whether the line parameters vary from night to night.

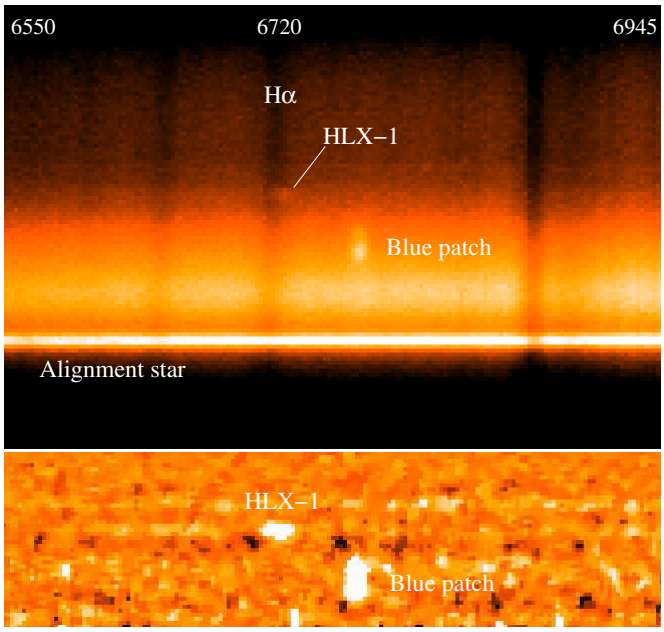

Figure 2. Top panel: two-dimensional spectrum in the Hα region (combined 2012 data), showing emission from HLX-1 and the candidate background galaxy (blue patch). The *X*-axis is the wavelength direction, and the *Y*-axis the spatial direction. The wavelength range is $\lambda = 6550$–6945 Å (as labeled at the top). An emission line from HLX-1 is apparent even before subtracting the stellar contribution from the halo of ESO 243−29. Note also that the HLX-1 emission feature is very close to but distinctly redshifted from the stellar Hα absorption line. Bottom panel: zoomed-in view of the emission features, plotted on the same wavelength scale as the panel above, after we have subtracted a model of the stellar spectrum from ESO 243−29. The image has been smoothed over 3 pixels. Hα from HLX-1 is centered at $\lambda \approx 6718.9$ Å (Section 4). The blue-patch line is unresolved (FWHM < 7.5 Å), centered at $\lambda \approx 6766.0$, corresponding to an apparent heliocentric recession velocity ≈9280 km s^{-1}, and a true velocity ≈9200 km s^{-1} after we correct for the offset from the slit center toward the red side (Figure 1).

(A color version of this figure is available in the online journal.)

The Hα emission is directly visible in the combined 2D spectra even before we subtract the stellar emission from ESO 243−49 (Figure 2, top panel). To obtain the galaxy-subtracted 2D spectra of HLX-1, we subtracted a model of the stellar emission, by fitting a second-order cubic spline function with 2σ rejection along the spatial direction. The resulting spectrum is shown in Figure 2 (bottom panel); note also the strong line emission from the candidate background galaxy (blue patch). Finally, we obtained one-dimensional spectra of HLX-1 by summing over 4 pixels (1″) in the spatial direction at each wavelength position along the slit (Figure 3).

4. MAIN RESULTS

4.1. Kinematics of HLX-1 and ESO 243−49

We confirm the presence of a strong emission line from HLX-1 (Figure 3), as discovered by Wiersema et al. (2010). We agree with Wiersema et al. (2010) that Hα is the most plausible identification for this line, given the characteristic recession velocities of ESO 243−49, and of the other galaxies in Abell 2877 (Malumuth et al. 1992). Henceforth, we shall assume this identification. From the 2012 data, we measured a central wavelength $\lambda \approx 6718.9 \pm 0.5 \pm 0.8$ Å; the errors are the statistical uncertainty and the systematic uncertainty in the wavelength solution (the latter is not relevant when we measure relative wavelength offsets). For the 2009 data, we

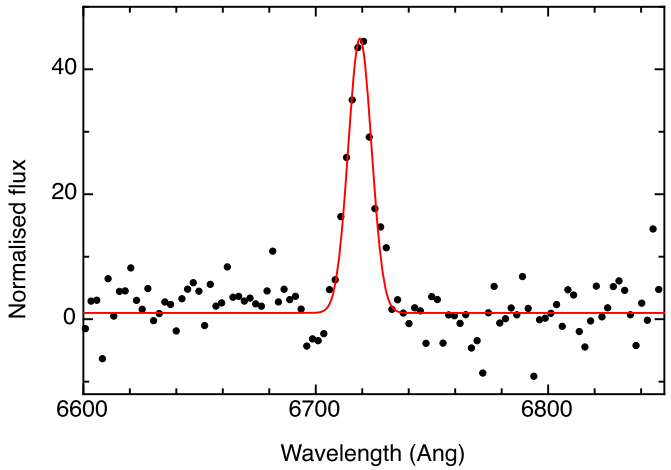

Figure 3. Normalized spectrum of the Hα spectral region in 2012, after subtraction of the galactic halo component, with a Gaussian fit to the emission line. The spectrum has been rebinned to a resolution of 2.44 Å pixel^{-1}.

(A color version of this figure is available in the online journal.)

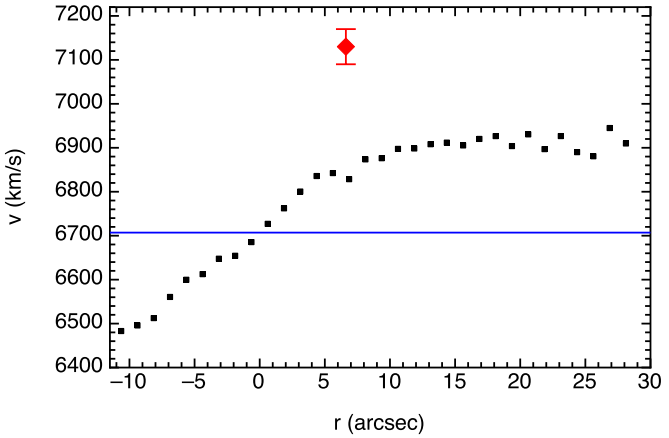

Figure 4. Rotation curve of ESO 243−49 along the slit, with the 2012 recession velocity of HLX-1 indicated by the red dot. The systemic velocity of ESO 243−49 is indicated by the blue line. On the *X*-axis, *r* increases from west to east.

(A color version of this figure is available in the online journal.)

measured $\lambda \approx 6717.6 \pm 0.7 \pm 0.8$ Å. This velocity difference ($\approx 60 \pm 40$ km s^{-1}) is almost certainly due to the offset position of HLX-1 in the slit in 2009, as expected. We take the 2012 measurement as the real line wavelength. The corresponding heliocentric recession velocity of HLX-1 is $v \approx 7131 \pm 22 \pm 35$ km s^{-1}; that is, a difference $\Delta v \approx 420$ km s^{-1} with respect to the recession velocity of the nucleus of ESO 243−49 reported in the literature (6714 ± 34 km s^{-1}; Caldwell & Rose 1997). The relative offset between the peaks of the Hα line emission and (stellar) absorption components at the location of HLX-1 is $\approx$6 Å.

To verify this interesting result, we determined the rotation curve of ESO 243−49 along the slit, although our observational setup was not specifically designed for rotational velocity measurements. We started by summing spectra in 1.″25 bins along the spatial direction. We then cross-correlated each of those galaxy spectra with a K2V template spectrum with solar metallicity (HD 149661; Valdes et al. 2004), using the *fxcor* task in the IRAF data analysis package. We restricted the cross-correlation to regions near the Hα and near-IR Ca II triplets. The resulting rotation curve along the slit is shown in Figure 4, where the center is defined as where the slit crosses the projected galaxy axis. The rotational velocity of ESO 243−49 is 209 ± 17 km s^{-1}, measured as the difference between the recession velocities at $r = 0$ and where the slit crosses the disk plane (at $r \approx 20''$). With this method, we confirm a heliocentric systemic velocity $\approx 6707 \pm 16 \pm 35$ km s^{-1} for ESO 243−49, and we conclude that HLX-1 is offset from it by 424 ± 27 km s^{-1}; HLX-1 is receding at a speed $\approx$215 km s^{-1} faster than the peak stellar rotational velocity, and $\approx$270 km s^{-1} faster than the stellar population seen projected around it in the D25 of ESO 243−49.

As a further check, we estimated the rotational velocity we should expect from a galaxy such as ESO 243−49, based on the Tully–Fisher relation (Williams et al. 2010; Tully & Fisher 1977). The total absolute brightness (corrected for extinction and *K*-correction) of ESO 243−49 is $M_B = -20.1 \pm 0.1$ mag, $M_{K_s} = -24.2 \pm 0.1$ mag (photometric measurements from the NASA/IPAC Extragalactic Database (NED) and Hyperleda databases). If we classify it as an Sa galaxy, the best-fitting Tully–Fisher relation gives a maximum rotational velocity $v_{\rm rot} = 210^{+30}_{-25}$ km s^{-1} from the *B*-band brightness, or 228^{+23}_{-22} km s^{-1} from the K_s-band brightness. If we classify it as an S0 galaxy, the Tully–Fisher relation predicts a best-fitting $v_{\rm rot} = 244^{+35}_{-30}$ km s^{-1}, or 259^{+27}_{-25} km s^{-1}, for the two bands, respectively. Considering the large scatter around the best-fitting Tully–Fisher relations, the rotational velocity we measured along the slit is in agreement with these expected rotational velocities and can be taken as a good approximation of the maximum rotational velocity.

The large velocity discrepancy proves that HLX-1 is kinematically decoupled from the stars at similar (projected) radial distances in ESO 243−49. This suggests that HLX-1 and its surrounding star cluster were not formed in situ, but originated either from a captured satellite or as a gravitational recoil from the nuclear region. We are unable to determine whether HLX-1 is bound or unbound to the galaxy—in the latter case it could be an intracluster IMBH. Determining the radial profile of the escape velocity requires detailed modeling of the gravitational potential from the light profile and 2D kinematics (which the current instrument setup is not designed for), and is beyond the scope of this Letter; in any case, this would not provide a definitive answer because we only know the projected position and radial velocity.

4.2. Width and Flux of the Hα Line

From the combined, background-subtracted 2012 spectrum, we measured a Gaussian FWHM $= 12.5 \pm 1.0$ Å for the Hα emission line. The instrumental line width inferred from the median seeing[4] is $\approx$7.8 Å; deconvolving it from the observed FWHM, we obtain that the line is resolved with an intrinsic FWHM $\approx (9.8 \pm 1.0)$ Å ≈ 440 km s^{-1}. However, when we consider only the average of the two nights with best seeing (2012 August 28 and September 11), we obtain an FWHM $= 10.3 \pm 1.2$ Å for a seeing-limited instrumental line width $\approx$7.4 Å; this corresponds to an intrinsic FWHM $= 7.2 \pm 1.2$ Å ≈ 320 km s^{-1}.

We estimate an integrated line flux of $(0.62 \pm 0.05) e^-$ s^{-1} in the combined 2012 spectrum. A faint continuum trace in the 2D spectra is visible by eye in a few exposures taken with excellent seeing ($\lesssim$0.″7). We mean-combined three 754 s exposures with the best signal-to-noise ratio (two from 2012 September 11

[4] From the sky lines, we determined that the fully illuminated slit gives an FWHM resolution of $\approx$9.9 Å; for a point-like source in the center of the slit, this value is then linearly scaled by the seeing, when it is $<1''$.

and one from 2012 August 28). We extracted the continuum from two spectral regions relatively free of interstellar lines, and excluding the Hα line itself: from 6420–6680 Å and from 6740–7065 Å; we averaged the measured values from the two bands, and obtained a continuum level of $(22 \pm 5)e^-$ pixel$^{-1} \approx (6.8 \pm 1.5)e^-$ Å^{-1}. This corresponds to an equivalent width (EW) of H$\alpha = (70 \pm 15)$ Å.

To convert the instrumental fluxes into physical units, we used the FORS2 Exposure Time Calculator. For a blackbody spectrum at $T \approx 15{,}000$–$20{,}000$ K, the continuum corresponds to $R = 24.5 \pm 0.5$ mag (Vega). The line flux is $f_{\rm H\alpha} = (2.0 \pm 0.3) \times 10^{-17}$ erg cm^{-2} s^{-1}, corresponding to a luminosity $\approx 2.3 \times 10^{37}$ erg s^{-1} (consistent with Wiersema et al. 2010).

Instead of using the somewhat uncertain (because of the rapidly changing background along the slit) optical flux calibrations, we could *assume* that the *R*-band continuum was the same as measured by *HST*/WFC3 on 2010 September 23, that is, $R \approx 23.7$ (Vegamag) ≈23.9 (ABmag; from Farrell et al. 2012; Mapelli et al. 2013, interpolated between F555W and F814W). In that case, for our measured EW, the line flux is $f_{\rm H\alpha} = (4.5 \pm 1.0) \times 10^{-17}$ erg cm^{-2} s^{-1}, corresponding to a luminosity $\approx 5.2 \times 10^{37}$ erg s^{-1}. However, there is still no proof that the optical/UV continuum flux is constant from epoch to epoch, as it is still debated whether it has a significant component from the irradiated accretion disk.

Galactic stellar-mass BHs often display Hα emission from the outer annuli of their accretion disks (e.g., Frank et al. 2002), with typical EW $\lesssim 10$ Å in the high-soft state and EW ∼ 10–100 Å during the decline toward quiescence (Fender et al. 2009). The exact value of the FWHM depends on the radial profile of the emissivity function (Smak 1981); however, for typical disk sizes and temperatures, if V_d is the rotational speed of the outermost annulus and i is the viewing angle, a useful first-order approximation is FWHM $\approx 2V_d \sin i$. In a Keplerian approximation, $V_d = (GM/R)^{1/2}$. For a BH mass $\sim 10^4\, M_\odot$ and an outer disk radius $\lesssim 10^{13}$ cm (Davis et al. 2011; Farrell et al. 2012; Soria et al. 2012; Soria 2013), we expect $V_d \gtrsim 3500$ km s^{-1} and FWHM $\gtrsim 7000(\sin i)$ km s^{-1}. Therefore, the narrow FWHM of the line observed from HLX-1 either requires an extremely face-on disk ($i \lesssim 3^\circ$) or, more likely, implies that the line does not come from a Keplerian disk. It might come, for example, from a larger X-ray photoionized nebula (XIN) around the BH, perhaps similar to those seen around some ultraluminous X-ray sources (ULXs; for example, RZ 2109 in NGC 4472: Peacock et al. 2012; Holmberg II X-1: Pakull & Mirioni 2002; Kaaret et al. 2004; Lehmann et al. 2005; NGC 5408 X-1: Kaaret & Corbel 2009) or stellar-mass BHs (LMC X-1; Pakull & Angebault 1986). Observations of those XINs, and models of line luminosities based on the photoionization code CLOUDY (Ferland et al. 2013), suggest that the Hα luminosity of an XIN is ≈0.3% of the (0.3–10) keV luminosity of the X-ray source. The exact value depends, among other parameters, on the detailed spectral energy distribution of the X-ray source and the nebular density, and should be considered to be indicative only within a factor of three. With this reservation in mind, we find that the Hα emission from HLX-1 could be excited by an X-ray luminosity of $\sim 1 \times 10^{40}$ erg s^{-1}, which is an order of magnitude smaller than the mean luminosity observed over 2009–2012. Possibly, the interstellar density is very small at the position of the X-ray source, or the emitting material has a low filling factor, or, alternatively, the mean luminosity of the source has indeed been lower in the past. Note that the Hα luminosity reflects the long-term-average X-ray luminosity over the recombination timescale $\tau = 1/[n_e\, \alpha(H^0, T)] \sim (10^5/n_e)$ yr, where α is the hydrogen recombination coefficient at temperature T, and n_e the electron density (Osterbrock 1989).

5. CONCLUSIONS

With our optical spectroscopic study, we have shown that HLX-1 has a high velocity offset $\Delta v_1 \approx 420$ km s^{-1} with respect to the galactic nucleus, and $\Delta v_2 \approx 270$ km s^{-1} with respect to the stellar rotational velocity at its projected location in the halo of ESO 243−49. We have also shown that the Hα emission line is resolved with an FWHM ≈ 400 km s^{-1}, a luminosity ≈ a few 10^{37} erg s^{-1}, and an EW ≈ 70 Å.

The kinematics of HLX-1 proves that it was not formed in situ: it is either the stripped remnant of a satellite dwarf (consistent with the simulations of Mapelli et al. 2012, 2013) or a recoiling BH ejected from the nucleus of ESO 243−49, dragging along a small, compact cluster of stars and gas inside its sphere of influence (Hoffman & Loeb 2006; Merritt et al. 2009). In the former case, it would have a very elongated, almost parabolic orbit (if bound at all to ESO 243−49). In the latter case, it may be unbound and destined to become soon (within ∼ few 10^7 yr) a free-floating intracluster IMBH. However, the recoiling BH scenario would be ruled out if most of the optical/UV emission came from a massive star cluster (Farrell et al. 2012) rather than an accretion disk.

Based on the large relative velocity of HLX-1, we speculate that there must exist other active IMBHs similar to HLX-1 not located or projected inside the D25 of a galaxy at the moment, either because they are on very eccentric orbits with large semimajor axes or because they have been ejected from a galaxy. Some of them may already have been observed in X-ray surveys but were perhaps misidentified and dismissed as background quasars, in the absence of any deep optical studies. We propose that a clue to identify those sources is an X-ray to optical flux ratio >100 (typical of IMBHs or stellar-mass BHs) associated with a soft X-ray spectrum and blue optical colors.

The small FWHM of Hα suggests that it does not come from the irradiated surface of a standard accretion disk. It is more likely to come from ionized gas at larger distances from the BH. This could be warm gas remaining in a young star cluster (age $\lesssim$ 5 Myr), or a nebula or outflow photoionized by the IMBH, similar to some ULX nebulae found in nearby galaxies. Deep long-slit observations in the blue region of the optical spectrum would provide a key test for the presence of other emission lines such as [O III] λ5007 and He II λ4686; in particular, the latter would provide strong indication of an ULX bubble.

R.S. acknowledges a Curtin University Senior Research Fellowship, and the hospitality of Marie-Claude Moery and of the Strasbourg Observatory. G.K.T.H. thanks ESO for the Director General's Discretionary Fund grant 12/18/C for this project, and the ESO staff who supported these observations. He also thanks the hospitality of Curtin University of Technology during his visit. We thank the referee for an insightful review, and Giovanni Carraro, Sean Farrell, Jeanette Gladstone, Alister Graham, James Miller-Jones, Michela Mapelli, Ivo Saviane, and Luca Zampieri for comments and suggestions.

REFERENCES

Caldwell, N., & Rose, J. A. 1997, AJ, 113, 492
Davis, S. W., Narayan, R., Zhu, Y., et al. 2011, ApJ, 734, 111

Farrell, S. A., Servillat, M., Pforr, J., et al. 2012, ApJL, 747, L13
Farrell, S. A., Webb, N. A., Barret, D., Godet, O., & Rodrigues, J. M. 2009, Natur, 460, 73
Fender, R. P., Russell, D. M., Knigge, C., et al. 2009, MNRAS, 393, 1608
Ferland, G. J., Porter, R. L., van Hoof, P. A. M., et al. 2013, RMxAA, 49, 137
Frank, J., King, A. R., & Raine, D. J. 2002, Accretion Power in Astrophysics (Cambridge: Cambridge Univ. Press)
Godet, O., Barret, D., Webb, N. A., Farrell, S. A., & Gehrels, N. 2009, ApJL, 705, L109
Godet, O., Webb, N., Barret, D., et al. 2012, ATel, 4327, 1
Hau, G. K. T., Carter, D., & Balcells, M. 1999, MNRAS, 306, 437
Hau, G. K. T., & Forbes, D. A. 2006, MNRAS, 371, 633
Hau, G. K. T., Spitler, L. R., Forbes, D. A., et al. 2009, MNRAS, 394, L97
Hoffman, L., & Loeb, A. 2006, ApJL, 638, L75
Kaaret, P., & Corbel, S. 2009, ApJ, 697, 950
Kaaret, P., Ward, M. J., & Zezas, A. 2004, MNRAS, 351, L83
Lasota, J.-P., Alexander, T., Dubus, G., et al. 2011, ApJ, 735, 89
Lehmann, I., Becker, T., Fabrika, S., et al. 2005, A&A, 431, 847
Malumuth, E. M., Kriss, G. A., Dixon, W. V. D., Ferguson, H. C., & Ritchie, C. 1992, AJ, 104, 495
Mapelli, M., Annibali, F., Zampieri, L., & Soria, R. 2013, MNRAS, submitted
Mapelli, M., Zampieri, L., & Mayer, L. 2012, MNRAS, 423, 1309
Merritt, D., Schnittman, J. D., & Komossa, S. 2009, ApJ, 699, 1690
Osterbrock, D. E. 1989, Astrophysics of Gaseous Nebulae and Active Galactic Nuclei (Mill Valley, CA: University Science Books)
Pakull, M. W., & Angebault, L. P. 1986, Natur, 322, 511
Pakull, M. W., & Mirioni, L. 2002, Online Proceedings of the Symposium on New Visions of the X-ray Universe in the *XMM-Newton* and *Chandra* Era, 2001 November 26–30, ESTEC, The Netherlands (arXiv:astro-ph/0202488)
Peacock, M. B., Zepf, S. E., Kundu, A., et al. 2012, ApJ, 759, 126
Planck Collaboration 2013, A&A, submitted (arXiv:1303.5076)
Servillat, M., Farrell, S. A., Lin, D., et al. 2011, ApJ, 743, 6
Smak, J. 1981, AcA, 31, 395
Soria, R. 2013, MNRAS, 428, 1944
Soria, R., Hakala, P. J., Hau, G. K. T., Gladstone, J. C., & Kong, A. K. H. 2012, MNRAS, 420, 3599
Soria, R., Hau, G. K. T., Graham, A. W., et al. 2010, MNRAS, 405, 870
Tully, R. B., & Fisher, J. R. 1977, A&A, 54, 661
Valdes, F., Gupta, R., Rose, J. A., Singh, H. P., & Bell, D. J. 2004, ApJS, 152, 251
Webb, N., Cseh, D., Lenc, E., et al. 2012, Sci, 337, 554
Wiersema, K., Farrell, S. A., Webb, N. A., et al. 2010, ApJL, 721, L102
Williams, M. J., Bureau, M., & Cappellari, M. 2010, MNRAS, 409, 1330